

CERN-EP-2022-121

07 June 2022

Observation of flow angle and flow magnitude fluctuations in Pb–Pb collisions at $\sqrt{s_{\text{NN}}} = 5.02$ TeV at the CERN Large Hadron Collider

ALICE Collaboration*

Abstract

This Letter reports on the first measurements of transverse momentum dependent flow angle Ψ_n and flow magnitude v_n fluctuations, determined using new four-particle correlators. The measurements are performed for various centralities in Pb–Pb collisions at a centre-of-mass energy per nucleon pair of $\sqrt{s_{\text{NN}}} = 5.02$ TeV with ALICE at the CERN Large Hadron Collider. Both flow angle and flow magnitude fluctuations are observed in the presented centrality ranges and are strongest in the most central collisions and for a transverse momentum $p_T > 2$ GeV/ c . Comparison with theoretical models, including iEBE-VISHNU, MUSIC, and AMPT, show that the measurements exhibit unique sensitivities to the initial state of heavy-ion collisions.

*See Appendix A for the list of collaboration members

In ultrarelativistic collisions of heavy ions, such as those at the BNL Relativistic Heavy-Ion Collider (RHIC) and the CERN Large Hadron Collider (LHC), a deconfined state of strongly interacting matter, commonly referred to as quark–gluon plasma (QGP), is predicted to be created under extreme conditions of temperature and energy densities [1, 2]. Many experimental results indicate that a strongly-coupled QGP is formed in heavy-ion collisions [3–7]. Initial anisotropies of the geometric overlap of the colliding nuclei and spatial inhomogeneities in the energy density drive the collective expansion of the QGP and are transformed through the evolution of the QGP into a momentum anisotropy in the final state [8–10]. This momentum anisotropy is characterised by a Fourier expansion of the distribution of the azimuthal angle, φ , of emitted particles [11]

$$\frac{d^2N}{dp_T d\varphi} = \frac{dN}{2\pi dp_T} \left(1 + 2 \sum_{n=1}^{\infty} v_n(p_T) \cos[n(\varphi - \Psi_n(p_T))] \right), \quad (1)$$

where $v_n(p_T)$ and $\Psi_n(p_T)$ correspond to the magnitude and angle, respectively, of the n^{th} -order harmonic flow vector $\vec{V}_n(p_T) = v_n(p_T)e^{in\Psi_n(p_T)}$. Here the transverse momentum, p_T , dependence of both the flow magnitude and flow angle has been made explicit. The flow vector quantifies the orientation and magnitude of the anisotropic flow, and the flow angle Ψ_n is the angle of the symmetry plane of the n^{th} -order flow vector.

Typically, the largest flow coefficient is the elliptic flow v_2 , since it is largely determined by the geometrical overlap of the colliding nuclei. However, fluctuations in the position of the colliding nuclei and in the position of nucleons within the nuclei can induce more complex geometrical shapes, which will give rise to non-zero flow coefficients with $n > 2$ [12–15], such as the triangular flow v_3 . Both elliptic and triangular flow coefficients have been measured extensively at RHIC [16–19] and the LHC [20–31]. The comparison to hydrodynamical calculations can constrain the initial conditions of the heavy-ion collisions and the transport properties of the QGP, such as the specific shear viscosity η/s . These comparisons indicate that the system behaves as a strongly-coupled low-viscosity fluid [10, 32–35].

Fluctuations of the flow angle Ψ_n and the flow magnitude v_n have been shown to be present in hydrodynamical models [36, 37]. These fluctuations are possibly due to thermal hydrodynamic fluctuations during the QGP evolution [38]. The *flow angle fluctuations* (FAF) are the fluctuations of $\Psi_n(p_T)$ determined by a subset of particles at a specific p_T with respect to the symmetry plane determined by the total set of particles, Ψ_n . If such fluctuations are present, $\Psi_n(p_T) \neq \Psi_n$. The *flow magnitude fluctuations* (FMF) of the v_n at different p_T can be understood as a decorrelation where $\langle v_n(p_T)v_n \rangle \neq \sqrt{\langle v_n^2(p_T) \rangle \langle v_n^2 \rangle}$.

The determination of QGP properties, such as η/s , rely on the comparison of theoretical model calculations to experimental data. In order to provide an unbiased extraction of the QGP properties, the models should account for the fluctuations in the flow angle and flow magnitude. Measurements at the LHC have reported the existence of p_T -dependent flow vector fluctuations [39–42]. However, those measurements rely on observables constructed from two-particle correlations, which intrinsically contain contributions from both the FAF and FMF with no way to separate the two experimentally.

In this Letter the FAF and FMF are measured with two new four-particle correlation functions to separate the components of the p_T -dependent fluctuations of the flow vector.

The FAF is quantified by

$$A_n^f = \frac{\langle \langle \cos n[\varphi_1^{\text{POI}} + \varphi_2^{\text{POI}} - \varphi_3 - \varphi_4] \rangle \rangle}{\langle \langle \cos n[\varphi_1^{\text{POI}} + \varphi_2 - \varphi_3^{\text{POI}} - \varphi_4] \rangle \rangle} = \frac{\langle v_n^2(p_T) v_n^2 \cos 2n[\Psi_n(p_T) - \Psi_n] \rangle}{\langle v_n^2(p_T) v_n^2 \rangle} \simeq \langle \cos 2n[\Psi_n(p_T) - \Psi_n] \rangle_w, \quad (2)$$

where the POI superscript refers to particles of interest selected from a narrow transverse momentum range and the w subscript means that A_n^f is averaged over the event ensemble with each event having a

weight equal to the fourth power of v_n [43]. The double brackets refer to an average over all particles and all events, and the single brackets refer to an average over all events. A value of $A_n^f < 1$ indicates the presence of p_T -dependent FAF. A large deviation from unity suggests that the symmetry plane at a specific p_T^{POI} deviates from the common symmetry plane.

The FMF are studied with

$$M_n^f = \frac{\langle\langle \cos n[\varphi_1^{\text{POI}} + \varphi_2 - \varphi_3^{\text{POI}} - \varphi_4] \rangle\rangle / (\langle\langle \cos n[\varphi_1^{\text{POI}} - \varphi_3^{\text{a}}] \rangle\rangle \langle\langle \cos n[\varphi_2 - \varphi_4] \rangle\rangle)}{\langle\langle \cos n[\varphi_1 + \varphi_2 - \varphi_3 - \varphi_4] \rangle\rangle / \langle\langle \cos n[\varphi_1 - \varphi_2] \rangle\rangle^2} = \frac{\langle v_n^2(p_T) v_n^2 \rangle / \langle v_n^2(p_T) \rangle \langle v_n^2 \rangle}{\langle v_n^4 \rangle / \langle v_n^2 \rangle^2}. \quad (3)$$

A deviation of M_n^f from unity indicates the presence of p_T -dependent FMF. The magnitude of the deviation will show how strongly the flow magnitude in a specific p_T range, $v_n(p_T)$, is decorrelated with respect to the integrated flow, v_n . The correlators A_n^f and M_n^f probe higher moments of the distribution of flow fluctuations compared to correlators traditionally used previously with two-particle techniques [39–41]. The lower-order moments of the FAF and FMF cannot be measured separately in experiments [36, 44] but can be approximated by constructing the lower and upper limits of the first moment of flow angle and magnitude fluctuations, respectively. The lower limit of the first-moment FAF $\langle \cos n[\Psi_n(p_T) - \Psi_n] \rangle$ is calculated with a double angle formula as

$$\sqrt{\frac{A_n^f + 1}{2}} \geq \langle \cos n[\Psi_n(p_T) - \Psi_n] \rangle. \quad (4)$$

The flow vector fluctuations are calculated as the ratio of the p_T -differential flow coefficient, defined as

$$v_n\{2\} = \frac{\langle\langle \cos n[\varphi_1^{\text{POI}} - \varphi_2] \rangle\rangle}{\langle\langle \cos n[\varphi_1 - \varphi_2] \rangle\rangle} = \frac{\langle v_n(p_T) v_n \cos n[\Psi_n(p_T) - \Psi_n] \rangle}{\sqrt{\langle v_n^2 \rangle}} \quad (5)$$

and the p_T -integrated flow coefficient in a narrow p_T interval [36], i.e.

$$v_n[2] = \langle\langle \cos n[\varphi_1^{\text{POI}} - \varphi_2^{\text{POI}}] \rangle\rangle = \sqrt{\langle v_n^2(p_T) \rangle}. \quad (6)$$

The flow vector fluctuations is then given by

$$v_n\{2\}/v_n[2] = \frac{\langle v_n(p_T) v_n \cos n[\Psi_n(p_T) - \Psi_n] \rangle}{\sqrt{\langle v_n^2(p_T) \rangle} \sqrt{\langle v_n^2 \rangle}}, \quad (7)$$

which satisfies the Cauchy-Schwartz inequality for two observables X and Y, $\langle XY \rangle \leq \sqrt{\langle X^2 \rangle \langle Y^2 \rangle}$, as $\cos n(\Psi_n(p_T) - \Psi_n) \leq 1$. The ratio of Eq. (4) and (7) determines the upper limit of the first-order FMF

$$\frac{v_n\{2\}/v_n[2]}{\sqrt{(A_n^f + 1)/2}} \leq \frac{\langle v_n(p_T) v_n \rangle}{\sqrt{\langle v_n^2(p_T) \rangle} \sqrt{\langle v_n^2 \rangle}}. \quad (8)$$

The limits on the first-moment flow angle and magnitude fluctuations connect the study of the separated fluctuations with prior studies of flow vector fluctuations based on two-particle correlations [39–41]. All the above correlators are calculated with the generic framework [45, 46], which corrects the non-uniformities in the acceptance of the detector. The statistical uncertainties of these two correlators in Eqs. (2) and (3) are estimated with the bootstrap method of random sampling with replacement.

The correlators A_2^f and M_2^f are measured based on 54 million Pb–Pb collisions recorded with the ALICE experiment [47] in 2015 at a centre-of-mass energy per nucleon pair of $\sqrt{s_{\text{NN}}} = 5.02$ TeV. Experimentally, events are selected based on a minimum bias trigger achieved by requiring a coincidence of signals in the

two V0 scintillator arrays, V0A with a pseudorapidity range $2.8 < \eta < 5.1$, and V0C with a pseudorapidity range $-3.7 < \eta < -1.7$. Additionally, a reconstructed primary vertex within ± 10 cm of the nominal interaction point along the beam axis is required. Events with significant pileup from out-of-bunch collisions within the Time Projection Chamber (TPC) readout time will have incorrect multiplicity and cannot be used to assess the collision properties of a given centrality class. Such pileup events are rejected based on cuts of the correlation between the number of tracks measured with different detectors. A variation of the criteria for pileup rejection is considered for the systematic uncertainties [48]. The centrality of the events is measured using information from the V0A and V0C detectors [49]. Charged particle tracks, hereafter simply called tracks, are reconstructed using the Inner Tracking System (ITS) [50] and the TPC [51]. Tracks are selected with at least 70 TPC space points out of 159 points and a χ^2 per TPC cluster less than 4 [52]. To reduce contamination from secondary particles, tracks are selected with a distance of closest approach to the primary vertex of less than 2 cm in the longitudinal direction and a p_T -dependent selection ranging from 0.2 cm at $p_T = 0.2$ GeV/c to 0.016 cm at $p_T = 5$ GeV/c in the transverse direction. Tracks are selected within the full TPC and ITS acceptance of $|\eta| < 0.8$. Additionally, as the regime of hard processes is not of interest in this work, the kinematic range of the tracks is restricted to $0.2 < p_T < 5$ GeV/c, where most of the tracks originate from the thermalised medium. In order to suppress non-flow correlation contributions, such as resonance decays and jets, which are not related to collective behaviour, the subevent method is utilised to calculate the correlators. In this method the event is divided into subevents separated by a gap in pseudorapidity denoted $|\Delta\eta|$. This ensures that short-range non-flow correlations between particles from the same subevent, mostly originating from resonances, are not introduced. An η -gap of $|\Delta\eta| > 0.8$ is used for two-particle correlations and $|\Delta\eta| > 0$ for four-particle correlations in order to ensure optimal balance between the statistical precision and non-flow suppression. To further investigate the non-flow suppression, the analysis is also performed with the so-called like-sign method, where only positively or negatively charged particle tracks are considered for analysis. The difference is less than 1% compared to the measurements of A_2^f and M_2^f using all tracks. Furthermore, the analysis is repeated with increasing pseudorapidity gaps between the subevents. Pseudorapidity gaps of $|\Delta\eta| > 0$, $|\Delta\eta| > 0.4$, and $|\Delta\eta| > 0.8$ are tested, and it is found that the measurements of A_2^f and M_2^f differ by less than 1%, when measured with different pseudorapidity gaps. Additional Monte Carlo studies using HIJING [53], a model that does not feature collective effects, but involves particle correlations arising from other sources, indicate that non-flow is sufficiently suppressed with the applied pseudorapidity gaps. The HIJING calculations of the four-particle correlation functions defined in Eqs. (2) and (3) show no statistically significant difference from zero. Based on the model studies, the like-sign method, and the variations of the pseudorapidity gaps, the non-flow correlation contributions are less than 1% of the measured values of A_2^f and M_2^f .

Systematic uncertainties are evaluated by varying the event and track selection criteria. The systematic uncertainty is presented for A_2^f , as the uncertainties are of a similar size for both observables. Since the systematic uncertainty may depend on the collision centrality and the p_T bin, only the largest contribution from each source is mentioned below. The systematic uncertainty associated with the event selection criteria is evaluated by varying the selection on the vertex position along the beam direction (from 10 cm to 7, 8, or 9 cm), the magnetic field polarity, and the criteria for rejecting pileup events, and is below 1%. The robustness of the centrality determination is investigated by repeating the analysis using the centrality estimated at midrapidity from hits in the Silicon Pixel Detector (SPD) instead of the V0, resulting in a negligible difference. Uncertainties related to track selection are estimated by considering different track reconstructions and track quality selection criteria. Changing the track reconstruction to include tracks without hits in the SPD leads to a variation of, at most, 1.7%. The quality of the reconstructed tracks is varied by changing the minimum number of TPC space points to 80 and 90, which leads to a difference of 1.5% on the measured correlators. Uncertainties related to the variations in the distance of closest approach in both longitudinal and transverse directions are negligible, indicating that the effect of contaminations from secondary particles on the measurements is insignificant. Finally, tightening the

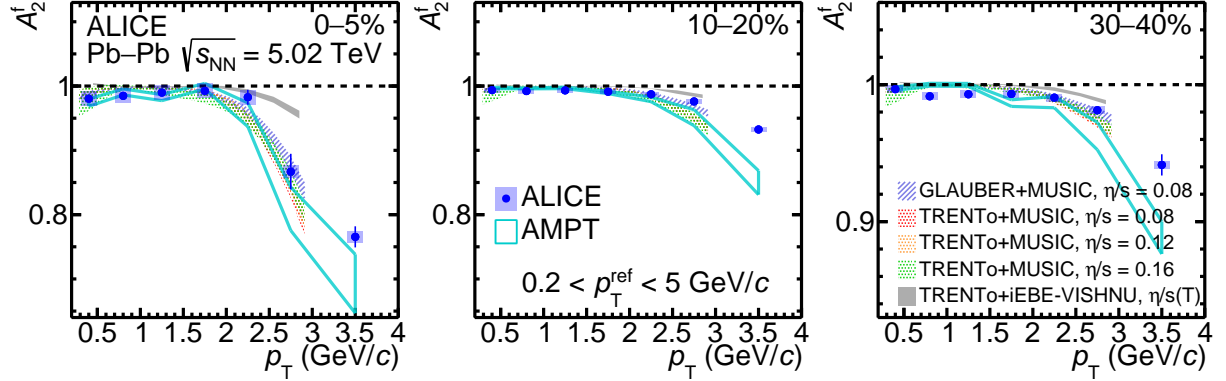


Figure 1: The flow angle fluctuation A_2^f in Pb–Pb collisions at $\sqrt{s_{\text{NN}}} = 5.02$ TeV as a function of the transverse momentum, p_T , in centrality classes 0–5% (left), 10–20% (middle), and 30–40% (right). Comparison with iEBE-VISHNU with T_RENTo initial conditions and $\eta/s(T)$ [55], MUSIC with Glauber initial conditions and $\eta/s = 0.08$ [56], MUSIC with T_RENTo initial conditions and $\eta/s = 0.08, 0.12, 0.16$ [56], and AMPT [57] are shown as coloured bands.

χ^2 per number of TPC clusters from 4 to 2.5 gives an uncertainty of, at most, 3%. The total systematic uncertainty is calculated as the quadratic sum of the individual sources that have a statistically significant contribution according to a statistical test [54].

Measured values of A_2^f are present in Fig. 1 as a function of the transverse momentum p_T in selected collision centrality classes. The results are presented from 0.2 GeV/c up to 4 GeV/c since the requirement of two particles at high p_T for the four-particle correlations limits the available data sample. In the 0–5% most central collisions, finite and increasing large deviations from unity are observed starting from $p_T \approx 2.5$ GeV/c. As previously mentioned, this deviation cannot be attributed to non-flow effects, whose contributions are negligible. With more than 5σ significance of the deviation at $p_T > 3$ GeV/c across the presented centralities, these measurements provide the first observation of p_T -dependent FAF. In centralities 10–20% and 30–40%, the fluctuation weakens in comparison to 0–5% most central collisions and reaches around 5–7% deviation from unity at $3 < p_T < 4$ GeV/c. The increasing deviation from unity with $p_T > 2.5$ GeV/c observed in data suggests that the elliptic flow at large transverse momentum ($p_T > 2.5$ GeV/c) may not be correlated with the reference flow and a common symmetry plane. This will affect the comparison of measurements relying on a common symmetry plane between particles at high and low p_T with theoretical models that do not feature FAF.

Theoretical calculations with AMPT [57, 58], MUSIC [59, 60], and iEBE-VISHNU [61] models are, when available, compared to the data in Fig. 1. The AMPT transport model uses partonic interactions within the string melting tune, while a quark coalescence model is utilised to form hadrons, which are then transported through a hadronic cascade model [62]. The input parameters of the AMPT model are tuned to measurements of $dN/d\eta$, p_T -spectra and elliptic flow of charged pions, kaons and protons from ALICE [57, 63]. On the other hand, the MUSIC model is an event-by-event (3+1D) viscous hydrodynamic model and is used with both Glauber [64] and T_RENTo [65] initial conditions. Different values of η/s of 0.08, 0.12, and 0.16 are used with T_RENTo initial conditions [56]. Finally, the iEBE-VISHNU model is an event-by-event (2+1D) viscous hydrodynamical model coupled to the hadronic cascade model UrQMD [66]. This model has been successful in describing collective phenomena, as well as event-by-event fluctuations, in several collision systems and energies [55, 67]. The iEBE-VISHNU model calculations with T_RENTo initial conditions and a temperature-dependent specific shear viscosity $\eta/s(T)$ [68] are also shown. The iEBE-VISHNU model calculations are available at p_T ranges below 3 GeV/c.

The AMPT calculation presented here describes the data well in the 0–5% most central collisions and

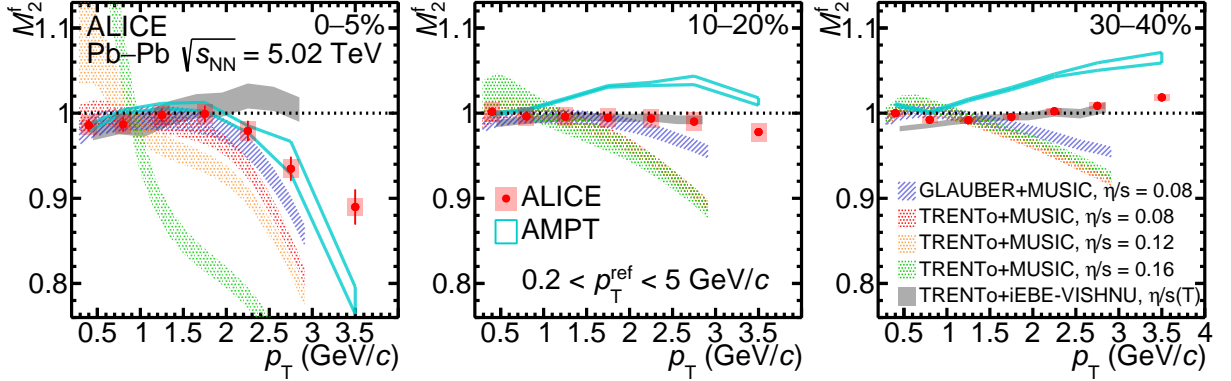


Figure 2: The flow magnitude fluctuation M_2^f in Pb–Pb collisions at $\sqrt{s_{\text{NN}}} = 5.02 \text{ TeV}$ as a function of the transverse momentum, p_T , in centrality classes 0–5% (left), 10–20% (middle), and 30–40% (right). Comparison with iEBE-VISHNU with T_RENTo initial conditions and $\eta/s(T)$ [55], MUSIC with Glauber initial conditions and $\eta/s = 0.08$ [56], MUSIC with T_RENTo initial conditions and $\eta/s = 0.08, 0.12, 0.16$ [56], and AMPT [57] are shown as coloured bands.

captures the deviation from unity in the highest p_T bin. At higher centralities, the AMPT calculation overestimates the deviation from unity at high p_T . The comparison of the MUSIC calculations with Glauber and T_RENTo initial conditions shows that A_2^f is sensitive to the fluctuations in the initial state with little to no sensitivity to the different values of specific shear viscosity. This observation is consistent with the AMPT calculations presented in [69], where AMPT with different values of specific shear viscosity and initial conditions are compared. The iEBE-VISHNU calculation underestimates the deviation of A_2^f from unity at $p_T > 2.5 \text{ GeV}/c$ across the presented centralities with the largest difference in the 0–5% most central collisions. The iEBE-VISHNU model with T_RENTo initial conditions uses parameters extracted from a Bayesian analysis [68] in contrast to the MUSIC models, which use standard T_RENTo initial conditions with $p = 0$ [65]. The extracted parameters from the Bayesian analysis represent the current best understanding of the initial conditions and QGP transport properties. Including additional constraints in the Bayesian analyses, such as A_2^f , should improve our understanding of the event-by-event fluctuating initial state thus allowing for a more robust and unbiased extraction of the expansion properties of the matter formed in these collisions.

The measurements of the p_T -dependent FMF, M_2^f in centrality classes 0–5%, 10–20%, and 30–40% are shown in Fig. 2. A substantial deviation of M_2^f from unity is observed in the 0–5% most central collisions. This deviation by more than 5σ significance at $p_T > 3 \text{ GeV}/c$ constitutes the first observation of p_T -dependent FMF. The measurements show that the p_T -differential flow coefficients decorrelate with the p_T -integrated flow coefficient as the transverse momentum increases. In centrality 0–5%, where the initial state fluctuations are most significant, the flow magnitude deviates from unity for p_T above $2 \text{ GeV}/c$. Deviations increase with rising p_T and are more pronounced in the 0–5% central collisions compared to those observed in the 10–20% and 30–40% centrality ranges. M_2^f is not restricted to be below unity as seen in Fig. 2 at 30–40% centrality. The observable M_n^f is not constructed to satisfy the Cauchy-Schwarz inequality as such an observable, $\langle v_n^2(p_T)v_n^2 \rangle / \sqrt{\langle v_n^4(p_T)v_n^4 \rangle}$, would require four particles from a narrow p_T range. The flow vector fluctuations measured with two-particle correlations and the FAF measured with A_2^f , however, can only be larger than unity due to non-flow effects [37]. The non-flow studies mentioned previously show that non-flow correlations are negligible for M_2^f , so the deviation from unity must be due to the FMF.

The AMPT transport model calculation succeeds in describing the FMF in the most central collisions, where it also describes the FAF (Fig. 1 left). At higher centralities, the AMPT model significantly overestimates the data even at low p_T , but it qualitatively captures the increasing trend of M_2^f in the 30–40% centrality interval. The AMPT model works well in qualitatively describing both FAF and FMF

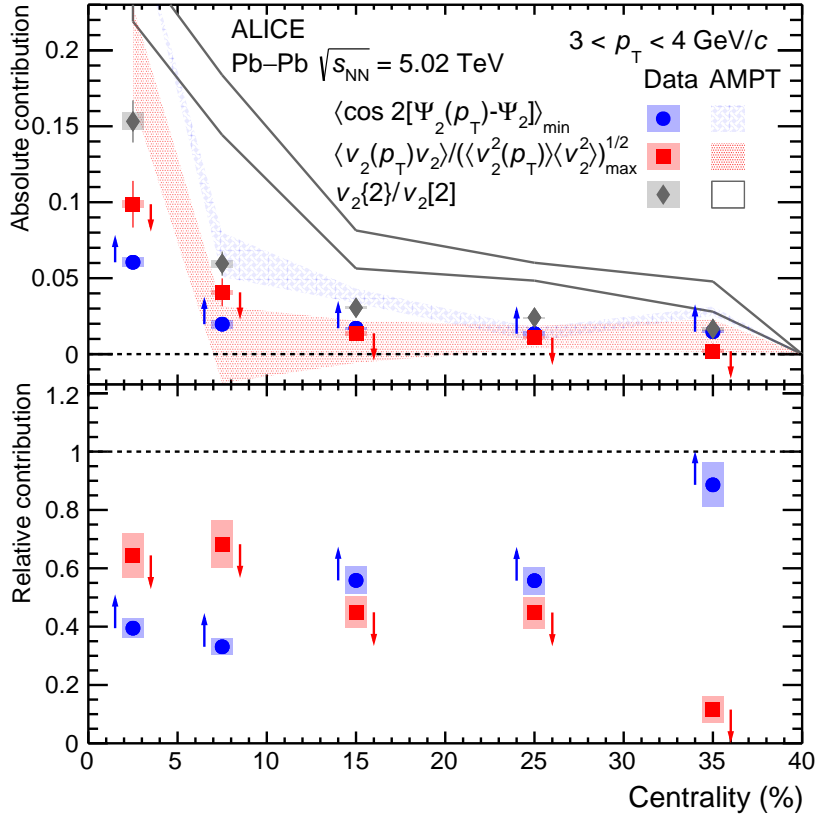


Figure 3: The lower limit of the first-order flow angle fluctuations, upper limit of the first-order flow magnitude fluctuations, and the flow vector fluctuations as a function of centrality for the $3.0 < p_T < 4.0 \text{ GeV}/c$. The lower and upper limits are denoted by the arrows. The top panel shows the absolute contribution and the bottom panel the contribution relative to the overall flow vector fluctuations. Comparisons to AMPT [57] are shown as coloured bands.

without a hydrodynamic phase. This is possibly due to the fact that these effects mainly originate in the initial state. The MUSIC models show strong sensitivity to the η/s in 0–5% most central collisions as well as a sensitivity to the different initial conditions. The dependence on η/s is unexpected and in contrast to the findings in [69], where the magnitude of the flow fluctuations is found to be independent of the value of η/s . In the 10–20% and 30–40% centrality intervals, M_2^f shows no sensitivity to η/s but is still affected by the different initial conditions. The MUSIC models overestimate the deviation of M_2^f from unity in all presented centrality classes. The iEBE-VISHNU calculations underestimate the effect in 0–5% centrality showing almost no p_T dependence. In the 10–20% and 30–40% centrality intervals, the model captures the increasing trend with p_T and, consequently, describes the data. The comparison of the measurements with the above models confirms that the FMF are driven by initial state fluctuations in non-central collisions. However, the dependence of M_2^f on η/s in the 0–5% central collisions with the MUSIC model is not well understood. The large discrepancy between the iEBE-VISHNU model and the data in central collisions suggests that the FMF could be an important observable in Bayesian analyses and could contribute further improvements of the extracted parameters used in the state-of-the-art description of the initial state and the QGP transport properties.

Equations (4) and (8) allow for the determination of the lower and upper limit for the contribution of the FAF and FMF, respectively, to the flow vector fluctuations defined in Eq. (7). Thus the lower moments of the FAF and FMF, which cannot be directly accessed in experiments, can be explored. The lower limit on the first-order FAF, the upper limit on the first-order FMF, and the total flow vector fluctuations are shown

as a function of centrality for the $3 < p_T < 4 \text{ GeV}/c$ range in Fig. 3. In central collisions, the upper limit on the FMF is higher than the lower limit of the FAF up to 10% centrality. For the 10–30% centrality interval, the limits are similar, and above 30% centrality, the flow magnitude upper limits are much smaller, and the FAF dominate the overall flow vector fluctuations completely. This is consistent with the measurements shown in Figs. 1 and 2, where M_2^f approaches unity faster with increasing centrality than A_2^f and even goes above unity in semicentral collisions. While p_T -dependent FAF and FMF are both present in central Pb–Pb collisions, the effects of FAF are present in all centralities considered in this work compared to the much smaller FMF in non-central collisions. The AMPT transport model calculations overestimate the flow vector fluctuations $v_2\{2\}/v_2[2]$ as well as the limits of the first-order FAF and FMF in the central collisions. At higher centralities, AMPT describes the lower and upper limits well, whereas the flow vector fluctuations are still overestimated by the model, as in central collisions. Hydrodynamic calculations for the limits are not available.

In summary, the p_T -dependent flow angle fluctuations and flow magnitude fluctuations of the second-order flow vector \vec{V}_2 are measured in Pb–Pb collisions at $\sqrt{s_{\text{NN}}} = 5.02 \text{ TeV}$ with the correlators A_2^f and M_2^f in centrality intervals 0–5%, 10–20%, and 30–40%. Large deviations from unity of both A_2^f ($\approx 20\%$) and M_2^f ($\approx 10\%$) are observed at $p_T > 3 \text{ GeV}/c$ in central collisions, where the event-by-event fluctuations of the position of the colliding nucleons dominate over the geometric response. In semicentral collisions, both flow angle and flow magnitude fluctuations decrease. The flow angle fluctuations reach 5–7%, and the flow magnitude fluctuations reach around 2% and are above unity in 30–40% centrality for the presented p_T range. The flow magnitude fluctuations decrease faster than the flow angle fluctuations up to 40% centrality, where the flow vector fluctuations are almost solely due to flow angle fluctuations. The comparison of the measurements to theoretical models shows that the observables are sensitive to the initial conditions of heavy-ion collisions. This suggests that the fluctuations originate during the early stages of the QGP evolution. The observation of flow angle and flow magnitude fluctuations thus gives additional insight into the nature of event-by-event fluctuations in the initial state of heavy-ion collisions and can be used to constrain the initial conditions and QGP properties.

Acknowledgments

The ALICE Collaboration would like to thank all its engineers and technicians for their invaluable contributions to the construction of the experiment and the CERN accelerator teams for the outstanding performance of the LHC complex. The ALICE Collaboration gratefully acknowledges the resources and support provided by all Grid centres and the Worldwide LHC Computing Grid (WLCG) collaboration. The ALICE Collaboration acknowledges the following funding agencies for their support in building and running the ALICE detector: A. I. Alikhanyan National Science Laboratory (Yerevan Physics Institute) Foundation (ANSL), State Committee of Science and World Federation of Scientists (WFS), Armenia; Austrian Academy of Sciences, Austrian Science Fund (FWF): [M 2467-N36] and Nationalstiftung für Forschung, Technologie und Entwicklung, Austria; Ministry of Communications and High Technologies, National Nuclear Research Center, Azerbaijan; Conselho Nacional de Desenvolvimento Científico e Tecnológico (CNPq), Financiadora de Estudos e Projetos (Finep), Fundação de Amparo à Pesquisa do Estado de São Paulo (FAPESP) and Universidade Federal do Rio Grande do Sul (UFRGS), Brazil; Bulgarian Ministry of Education and Science, within the National Roadmap for Research Infrastructures 2020–2027 (object CERN), Bulgaria; Ministry of Education of China (MOEC), Ministry of Science & Technology of China (MSTC) and National Natural Science Foundation of China (NSFC), China; Ministry of Science and Education and Croatian Science Foundation, Croatia; Centro de Aplicaciones Tecnológicas y Desarrollo Nuclear (CEADEN), Cubaenergía, Cuba; Ministry of Education, Youth and Sports of the Czech Republic, Czech Republic; The Danish Council for Independent Research | Natural Sciences, the VILLUM FONDEN and Danish National Research Foundation (DNRF), Denmark; Helsinki Institute of Physics (HIP), Finland; Commissariat à l’Energie Atomique (CEA) and

Institut National de Physique Nucléaire et de Physique des Particules (IN2P3) and Centre National de la Recherche Scientifique (CNRS), France; Bundesministerium für Bildung und Forschung (BMBF) and GSI Helmholtzzentrum für Schwerionenforschung GmbH, Germany; General Secretariat for Research and Technology, Ministry of Education, Research and Religions, Greece; National Research, Development and Innovation Office, Hungary; Department of Atomic Energy Government of India (DAE), Department of Science and Technology, Government of India (DST), University Grants Commission, Government of India (UGC) and Council of Scientific and Industrial Research (CSIR), India; National Research and Innovation Agency - BRIN, Indonesia; Istituto Nazionale di Fisica Nucleare (INFN), Italy; Japanese Ministry of Education, Culture, Sports, Science and Technology (MEXT) and Japan Society for the Promotion of Science (JSPS) KAKENHI, Japan; Consejo Nacional de Ciencia (CONACYT) y Tecnología, through Fondo de Cooperación Internacional en Ciencia y Tecnología (FONCICYT) and Dirección General de Asuntos del Personal Académico (DGAPA), Mexico; Nederlandse Organisatie voor Wetenschappelijk Onderzoek (NWO), Netherlands; The Research Council of Norway, Norway; Commission on Science and Technology for Sustainable Development in the South (COMSATS), Pakistan; Pontificia Universidad Católica del Perú, Peru; Ministry of Education and Science, National Science Centre and WUT ID-UB, Poland; Korea Institute of Science and Technology Information and National Research Foundation of Korea (NRF), Republic of Korea; Ministry of Education and Scientific Research, Institute of Atomic Physics, Ministry of Research and Innovation and Institute of Atomic Physics and University Politehnica of Bucharest, Romania; Ministry of Education, Science, Research and Sport of the Slovak Republic, Slovakia; National Research Foundation of South Africa, South Africa; Swedish Research Council (VR) and Knut & Alice Wallenberg Foundation (KAW), Sweden; European Organization for Nuclear Research, Switzerland; Suranaree University of Technology (SUT), National Science and Technology Development Agency (NSTDA), Thailand Science Research and Innovation (TSRI) and National Science, Research and Innovation Fund (NSRF), Thailand; Turkish Energy, Nuclear and Mineral Research Agency (TENMAK), Turkey; National Academy of Sciences of Ukraine, Ukraine; Science and Technology Facilities Council (STFC), United Kingdom; National Science Foundation of the United States of America (NSF) and United States Department of Energy, Office of Nuclear Physics (DOE NP), United States of America. In addition, individual groups or members have received support from: Marie Skłodowska Curie, European Research Council, Strong 2020 - Horizon 2020 (grant nos. 950692, 824093, 896850), European Union; Academy of Finland (Center of Excellence in Quark Matter) (grant nos. 346327, 346328), Finland; Programa de Apoyos para la Superación del Personal Académico, UNAM, Mexico.

References

- [1] E. V. Shuryak, “Quark-Gluon Plasma and Hadronic Production of Leptons, Photons and Psions”, *Phys. Lett.* **B78** (1978) 150. [Yad. Fiz.28,796(1978)].
- [2] E. V. Shuryak, “Quantum Chromodynamics and the Theory of Superdense Matter”, *Phys. Rept.* **61** (1980) 71–158.
- [3] **BRAHMS** Collaboration, I. Arsene *et al.*, “Quark gluon plasma and color glass condensate at RHIC? The Perspective from the BRAHMS experiment”, *Nucl. Phys. A* **757** (2005) 1–27, arXiv:nucl-ex/0410020.
- [4] **STAR** Collaboration, J. Adams *et al.*, “Experimental and theoretical challenges in the search for the quark gluon plasma: The STAR Collaboration’s critical assessment of the evidence from RHIC collisions”, *Nucl. Phys. A* **757** (2005) 102–183, arXiv:nucl-ex/0501009.
- [5] **PHENIX** Collaboration, K. Adcox *et al.*, “Formation of dense partonic matter in relativistic nucleus-nucleus collisions at RHIC: Experimental evaluation by the PHENIX collaboration”, *Nucl. Phys. A* **757** (2005) 184–283, arXiv:nucl-ex/0410003.

- [6] **PHOBOS** Collaboration, B. B. Back *et al.*, “The PHOBOS perspective on discoveries at RHIC”, *Nucl. Phys. A* **757** (2005) 28–101, arXiv:nucl-ex/0410022.
- [7] B. Muller, J. Schukraft, and B. Wyslouch, “First Results from Pb+Pb collisions at the LHC”, *Ann. Rev. Nucl. Part. Sci.* **62** (2012) 361–386, arXiv:1202.3233 [hep-ex].
- [8] J.-Y. Ollitrault, “Anisotropy as a signature of transverse collective flow”, *Phys. Rev.* **D46** (1992) 229–245.
- [9] S. A. Voloshin, A. M. Poskanzer, and R. Snellings, “Collective phenomena in non-central nuclear collisions”, *Landolt-Bornstein* **23** (2010) 293–333, arXiv:0809.2949 [nucl-ex].
- [10] U. Heinz and R. Snellings, “Collective flow and viscosity in relativistic heavy-ion collisions”, *Ann. Rev. Nucl. Part. Sci.* **63** (2013) 123–151, arXiv:1301.2826 [nucl-th].
- [11] S. Voloshin and Y. Zhang, “Flow study in relativistic nuclear collisions by Fourier expansion of Azimuthal particle distributions”, *Z. Phys.* **C70** (1996) 665–672, arXiv:hep-ph/9407282 [hep-ph].
- [12] B. Alver and G. Roland, “Collision geometry fluctuations and triangular flow in heavy-ion collisions”, *Phys. Rev.* **C81** (2010) 054905, arXiv:1003.0194 [nucl-th]. [Erratum: Phys. Rev.C82,039903(2010)].
- [13] B. H. Alver, C. Gombeaud, M. Luzum, and J.-Y. Ollitrault, “Triangular flow in hydrodynamics and transport theory”, *Phys. Rev.* **C82** (2010) 034913, arXiv:1007.5469 [nucl-th].
- [14] D. Teaney and L. Yan, “Triangularity and Dipole Asymmetry in Heavy Ion Collisions”, *Phys. Rev.* **C83** (2011) 064904, arXiv:1010.1876 [nucl-th].
- [15] M. Luzum, “Collective flow and long-range correlations in relativistic heavy ion collisions”, *Phys. Lett.* **B696** (2011) 499–504, arXiv:1011.5773 [nucl-th].
- [16] **STAR** Collaboration, K. H. Ackermann *et al.*, “Elliptic flow in Au + Au collisions at $(S(NN))^{**}(1/2) = 130 \text{ GeV}$ ”, *Phys. Rev. Lett.* **86** (2001) 402–407, arXiv:nucl-ex/0009011.
- [17] **PHENIX** Collaboration, S. S. Adler *et al.*, “Elliptic flow of identified hadrons in Au+Au collisions at $s(NN)^{**}(1/2) = 200\text{-GeV}$ ”, *Phys. Rev. Lett.* **91** (2003) 182301, arXiv:nucl-ex/0305013.
- [18] **STAR** Collaboration, L. Adamczyk *et al.*, “Third Harmonic Flow of Charged Particles in Au+Au Collisions at $\sqrt{s_{NN}} = 200 \text{ GeV}$ ”, *Phys. Rev. C* **88** (2013) 014904, arXiv:1301.2187 [nucl-ex].
- [19] **PHENIX** Collaboration, A. Adare *et al.*, “Measurements of elliptic and triangular flow in high-multiplicity ${}^3\text{He}+\text{Au}$ collisions at $\sqrt{s_{NN}} = 200 \text{ GeV}$ ”, *Phys. Rev. Lett.* **115** (2015) 142301, arXiv:1507.06273 [nucl-ex].
- [20] **ALICE** Collaboration, K. Aamodt *et al.*, “Elliptic flow of charged particles in Pb-Pb collisions at 2.76 TeV”, *Phys. Rev. Lett.* **105** (2010) 252302, arXiv:1011.3914 [nucl-ex].
- [21] **ALICE** Collaboration, K. Aamodt *et al.*, “Higher harmonic anisotropic flow measurements of charged particles in Pb-Pb collisions at $\sqrt{s_{NN}}=2.76 \text{ TeV}$ ”, *Phys. Rev. Lett.* **107** (2011) 032301, arXiv:1105.3865 [nucl-ex].
- [22] **ALICE** Collaboration, B. Abelev *et al.*, “Elliptic flow of identified hadrons in Pb-Pb collisions at $\sqrt{s_{NN}} = 2.76 \text{ TeV}$ ”, *JHEP* **06** (2015) 190, arXiv:1405.4632 [nucl-ex].

- [23] ALICE Collaboration, J. Adam *et al.*, “Anisotropic flow of charged particles in Pb-Pb collisions at $\sqrt{s_{NN}} = 5.02$ TeV”, *Phys. Rev. Lett.* **116** (2016) 132302, arXiv:1602.01119 [nucl-ex].
- [24] ALICE Collaboration, S. Acharya *et al.*, “Linear and non-linear flow modes in Pb-Pb collisions at $\sqrt{s_{NN}} = 2.76$ TeV”, *Phys. Lett.* **B773** (2017) 68–80, arXiv:1705.04377 [nucl-ex].
- [25] ATLAS Collaboration, G. Aad *et al.*, “Measurement of the azimuthal anisotropy for charged particle production in $\sqrt{s_{NN}} = 2.76$ TeV lead-lead collisions with the ATLAS detector”, *Phys. Rev.* **C86** (2012) 014907, arXiv:1203.3087 [hep-ex].
- [26] ATLAS Collaboration, G. Aad *et al.*, “Measurement of the pseudorapidity and transverse momentum dependence of the elliptic flow of charged particles in lead-lead collisions at $\sqrt{s_{NN}} = 2.76$ TeV with the ATLAS detector”, *Phys. Lett.* **B707** (2012) 330–348, arXiv:1108.6018 [hep-ex].
- [27] ATLAS Collaboration, G. Aad *et al.*, “Measurement of the distributions of event-by-event flow harmonics in lead-lead collisions at $\sqrt{s_{NN}} = 2.76$ TeV with the ATLAS detector at the LHC”, *JHEP* **11** (2013) 183, arXiv:1305.2942 [hep-ex].
- [28] CMS Collaboration, S. Chatrchyan *et al.*, “Centrality dependence of dihadron correlations and azimuthal anisotropy harmonics in PbPb collisions at $\sqrt{s_{NN}} = 2.76$ TeV”, *Eur. Phys. J.* **C72** (2012) 2012, arXiv:1201.3158 [nucl-ex].
- [29] CMS Collaboration, S. Chatrchyan *et al.*, “Measurement of the elliptic anisotropy of charged particles produced in PbPb collisions at $\sqrt{s_{NN}} = 2.76$ TeV”, *Phys. Rev.* **C87** (2013) 014902, arXiv:1204.1409 [nucl-ex].
- [30] CMS Collaboration, S. Chatrchyan *et al.*, “Azimuthal anisotropy of charged particles at high transverse momenta in PbPb collisions at $\sqrt{s_{NN}} = 2.76$ TeV”, *Phys. Rev. Lett.* **109** (2012) 022301, arXiv:1204.1850 [nucl-ex].
- [31] ALICE Collaboration, S. Acharya *et al.*, “Anisotropic flow in Xe-Xe collisions at $\sqrt{s_{NN}} = 5.44$ TeV”, *Phys. Lett. B* **784** (2018) 82–95, arXiv:1805.01832 [nucl-ex].
- [32] M. Luzum and H. Petersen, “Initial State Fluctuations and Final State Correlations in Relativistic Heavy-Ion Collisions”, *J. Phys.* **G41** (2014) 063102, arXiv:1312.5503 [nucl-th].
- [33] E. Shuryak, “Strongly coupled quark-gluon plasma in heavy ion collisions”, *Rev. Mod. Phys.* **89** (2017) 035001, arXiv:1412.8393 [hep-ph].
- [34] H. Song, Y. Zhou, and K. Gajdosova, “Collective flow and hydrodynamics in large and small systems at the LHC”, *Nucl. Sci. Tech.* **28** (2017) 99, arXiv:1703.00670 [nucl-th].
- [35] ALICE Collaboration, “The ALICE experiment – A journey through QCD”, arXiv:2211.04384 [nucl-ex].
- [36] U. Heinz, Z. Qiu, and C. Shen, “Fluctuating flow angles and anisotropic flow measurements”, *Phys. Rev.* **C87** (2013) 034913, arXiv:1302.3535 [nucl-th].
- [37] F. G. Gardim, F. Grassi, M. Luzum, and J.-Y. Ollitrault, “Breaking of factorization of two-particle correlations in hydrodynamics”, *Phys. Rev.* **C87** (2013) 031901, arXiv:1211.0989 [nucl-th].
- [38] A. Sakai, K. Murase, and T. Hirano, “Rapidity decorrelation of anisotropic flow caused by hydrodynamic fluctuations”, *Phys. Rev. C* **102** (2020) 064903, arXiv:2003.13496 [nucl-th].

- [39] ALICE Collaboration, S. Acharya *et al.*, “Searches for transverse momentum dependent flow vector fluctuations in Pb-Pb and p-Pb collisions at the LHC”, *JHEP* **09** (2017) 032, arXiv:1707.05690 [nucl-ex].
- [40] CMS Collaboration, S. Chatrchyan *et al.*, “Studies of azimuthal dihadron correlations in ultra-central PbPb collisions at $\sqrt{s_{NN}} = 2.76$ TeV”, *JHEP* **02** (2014) 088, arXiv:1312.1845 [nucl-ex].
- [41] CMS Collaboration, V. Khachatryan *et al.*, “Evidence for transverse momentum and pseudorapidity dependent event plane fluctuations in PbPb and pPb collisions”, *Phys. Rev.* **C92** (2015) 034911, arXiv:1503.01692 [nucl-ex].
- [42] ALICE Collaboration, K. Aamodt *et al.*, “Harmonic decomposition of two-particle angular correlations in Pb-Pb collisions at $\sqrt{s_{NN}} = 2.76$ TeV”, *Phys. Lett.* **B708** (2012) 249–264, arXiv:1109.2501 [nucl-ex].
- [43] P. Bozek and W. Broniowski, “Longitudinal decorrelation measures of flow magnitude and event-plane angles in ultrarelativistic nuclear collisions”, *Phys. Rev. C* **97** (2018) 034913, arXiv:1711.03325 [nucl-th].
- [44] P. Božek and R. Samanta, “Higher order cumulants of transverse momentum and harmonic flow in relativistic heavy ion collisions”, *Phys. Rev. C* **104** (2021) 014905, arXiv:2103.15338 [nucl-th].
- [45] A. Bilandzic, C. H. Christensen, K. Gulbrandsen, A. Hansen, and Y. Zhou, “Generic framework for anisotropic flow analyses with multiparticle azimuthal correlations”, *Phys. Rev.* **C89** (2014) 064904, arXiv:1312.3572 [nucl-ex].
- [46] Z. Moravcova, K. Gulbrandsen, and Y. Zhou, “Generic algorithm for multiparticle cumulants of azimuthal correlations in high energy nucleus collisions”, *Phys. Rev.* **C103** (2021) 024913, arXiv:2005.07974 [nucl-th].
- [47] ALICE Collaboration, K. Aamodt *et al.*, “The ALICE experiment at the CERN LHC”, *JINST* **3** (2008) S08002.
- [48] ALICE Collaboration, B. Abelev *et al.*, “Performance of the ALICE Experiment at the CERN LHC”, *Int. J. Mod. Phys.* **A29** (2014) 1430044, arXiv:1402.4476 [nucl-ex].
- [49] ALICE Collaboration, B. Abelev *et al.*, “Centrality determination of Pb-Pb collisions at $\sqrt{s_{NN}} = 2.76$ TeV with ALICE”, *Phys. Rev.* **C88** (2013) 044909, arXiv:1301.4361 [nucl-ex].
- [50] ALICE Collaboration, K. Aamodt *et al.*, “Alignment of the ALICE Inner Tracking System with cosmic-ray tracks”, *JINST* **5** (2010) P03003, arXiv:1001.0502 [physics.ins-det].
- [51] J. Alme *et al.*, “The ALICE TPC, a large 3-dimensional tracking device with fast readout for ultra-high multiplicity events”, *Nucl. Instrum. Meth.* **A622** (2010) 316–367, arXiv:1001.1950 [physics.ins-det].
- [52] ALICE Collaboration, “The ALICE definition of primary particles”, *ALICE-PUBLIC-2017-005* (Jun, 2017) . <https://cds.cern.ch/record/2270008>.
- [53] X.-N. Wang and M. Gyulassy, “hijing: A monte carlo model for multiple jet production in pp, pA, and AA collisions”, *Phys. Rev.* **D44** (Dec, 1991) 3501–3516.
- [54] R. Barlow, “Systematic errors: Facts and fictions”, in *Conference on Advanced Statistical Techniques in Particle Physics*, pp. 134–144. 7, 2002. arXiv:hep-ex/0207026.

- [55] W. Zhao, H.-j. Xu, and H. Song, “Collective flow in 2.76 A TeV and 5.02 A TeV Pb+Pb collisions”, *Eur. Phys. J.* **C77** (2017) 645, arXiv:1703.10792 [nucl-th].
- [56] P. Bozek and R. Samanta, “Factorization breaking for higher moments of harmonic flow”, *Phys. Rev. C* **105** (2022) 034904, arXiv:2109.07781 [nucl-th].
- [57] G.-L. Ma and Z.-W. Lin, “Predictions for $\sqrt{s_{NN}} = 5.02$ TeV Pb+Pb Collisions from a Multi-Phase Transport Model”, *Phys. Rev.* **C93** (2016) 054911, arXiv:1601.08160 [nucl-th].
- [58] Z.-W. Lin, C. M. Ko, B.-A. Li, B. Zhang, and S. Pal, “A Multi-phase transport model for relativistic heavy ion collisions”, *Phys. Rev.* **C72** (2005) 064901, arXiv:nucl-th/0411110 [nucl-th].
- [59] B. Schenke, S. Jeon, and C. Gale, “Elliptic and triangular flow in event-by-event (3+1)D viscous hydrodynamics”, *Phys. Rev. Lett.* **106** (2011) 042301, arXiv:1009.3244 [hep-ph].
- [60] B. Schenke, S. Jeon, and C. Gale, “(3+1)D hydrodynamic simulation of relativistic heavy-ion collisions”, *Phys. Rev.* **C82** (2010) 014903, arXiv:1004.1408 [hep-ph].
- [61] C. Shen, Z. Qiu, H. Song, J. Bernhard, S. Bass, and U. Heinz, “The iEBE-VISHNU code package for relativistic heavy-ion collisions”, *Comput. Phys. Commun.* **199** (2016) 61–85, arXiv:1409.8164 [nucl-th].
- [62] B.-A. Li and C. M. Ko, “Formation of superdense hadronic matter in high-energy heavy ion collisions”, *Phys. Rev.* **C52** (1995) 2037–2063, arXiv:nucl-th/9505016 [nucl-th].
- [63] J. Xu and C. M. Ko, “Pb-Pb collisions at $\sqrt{s_{NN}} = 2.76$ TeV in a multiphase transport model”, *Phys. Rev. C* **83** (2011) 034904, arXiv:1101.2231 [nucl-th].
- [64] P. Božek, W. Broniowski, M. Rybczynski, and G. Stefanek, “GLISSANDO 3: GLauber Initial-State Simulation AND mOre..., ver. 3”, *Comput. Phys. Commun.* **245** (2019) 106850, arXiv:1901.04484 [nucl-th].
- [65] J. S. Moreland, J. E. Bernhard, and S. A. Bass, “Alternative ansatz to wounded nucleon and binary collision scaling in high-energy nuclear collisions”, *Phys. Rev.* **C92** (2015) 011901, arXiv:1412.4708 [nucl-th].
- [66] S. A. Bass *et al.*, “Microscopic models for ultrarelativistic heavy ion collisions”, *Prog. Part. Nucl. Phys.* **41** (1998) 255–369, arXiv:nucl-th/9803035 [nucl-th].
- [67] M. Li, Y. Zhou, W. Zhao, B. Fu, Y. Mou, and H. Song, “Investigations on mixed harmonic cumulants in heavy-ion collisions at energies available at the CERN Large Hadron Collider”, *Phys. Rev.* **C104** (2021) 024903, arXiv:2104.10422 [nucl-th].
- [68] J. E. Bernhard, J. S. Moreland, S. A. Bass, J. Liu, and U. Heinz, “Applying Bayesian parameter estimation to relativistic heavy-ion collisions: simultaneous characterization of the initial state and quark-gluon plasma medium”, *Phys. Rev.* **C94** (2016) 024907, arXiv:1605.03954 [nucl-th].
- [69] E. G. Nielsen and Y. Zhou, “Transverse momentum decorrelation of the flow vector in Pb-Pb collisions at $\sqrt{s_{NN}} = 5.02$ TeV”, arXiv:2211.13651 [nucl-ex].

A The ALICE Collaboration

- S. Acharya ^{125,132}, D. Adamová ⁸⁶, A. Adler⁶⁹, G. Aglieri Rinella ³², M. Agnello ²⁹, N. Agrawal ⁵⁰, Z. Ahammed ¹³², S. Ahmad ¹⁵, S.U. Ahn ⁷⁰, I. Ahuja ³⁷, A. Akindinov ¹⁴⁰, M. Al-Turany ⁹⁸, D. Aleksandrov ¹⁴⁰, B. Alessandro ⁵⁵, H.M. Alfanda ⁶, R. Alfaro Molina ⁶⁶, B. Ali ¹⁵, Y. Ali ¹³, A. Alici ²⁵, N. Alizadehvandchali ¹¹⁴, A. Alkin ³², J. Alme ²⁰, G. Alocco ⁵¹, T. Alt ⁶³, I. Altsybeev ¹⁴⁰, M.N. Anaam ⁶, C. Andrei ⁴⁵, A. Andronic ¹³⁵, V. Anguelov ⁹⁵, F. Antinori ⁵³, P. Antonioli ⁵⁰, C. Anuj ¹⁵, N. Apadula ⁷⁴, L. Aphecetche ¹⁰⁴, H. Appelshäuser ⁶³, C. Arata ⁷³, S. Arcelli ²⁵, M. Aresti ⁵¹, R. Arnaldi ⁵⁵, I.C. Arsene ¹⁹, M. Arslanbekov ¹³⁷, A. Augustinus ³², R. Averbeck ⁹⁸, S. Aziz ⁷², M.D. Azmi ¹⁵, A. Badalà ⁵², Y.W. Baek ⁴⁰, X. Bai ¹¹⁸, R. Bailhache ⁶³, Y. Bailung ⁴⁷, R. Bala ⁹¹, A. Balbino ²⁹, A. Baldissari ¹²⁸, B. Balis ², D. Banerjee ⁴, Z. Banoo ⁹¹, R. Barbera ²⁶, L. Barioglio ⁹⁶, M. Barlou ⁷⁸, G.G. Barnaföldi ¹³⁶, L.S. Barnby ⁸⁵, V. Barret ¹²⁵, L. Barreto ¹¹⁰, C. Bartels ¹¹⁷, K. Barth ³², E. Bartsch ⁶³, F. Baruffaldi ²⁷, N. Bastid ¹²⁵, S. Basu ⁷⁵, G. Batigne ¹⁰⁴, D. Battistini ⁹⁶, B. Batyunya ¹⁴¹, D. Bauri ⁴⁶, J.L. Bazo Alba ¹⁰², I.G. Bearden ⁸³, C. Beattie ¹³⁷, P. Becht ⁹⁸, D. Behera ⁴⁷, I. Belikov ¹²⁷, A.D.C. Bell Hechavarria ¹³⁵, F. Bellini ²⁵, R. Bellwied ¹¹⁴, S. Belokurova ¹⁴⁰, V. Belyaev ¹⁴⁰, G. Bencedi ^{136,64}, S. Beole ²⁴, A. Bercuci ⁴⁵, Y. Berdnikov ¹⁴⁰, A. Berdnikova ⁹⁵, L. Bergmann ⁹⁵, M.G. Besouï ⁶², L. Betev ³², P.P. Bhaduri ¹³², A. Bhasin ⁹¹, M.A. Bhat ⁴, B. Bhattacharjee ⁴¹, L. Bianchi ²⁴, N. Bianchi ⁴⁸, J. Bielčík ³⁵, J. Bielčíková ⁸⁶, J. Biernat ¹⁰⁷, A.P. Bigot ¹²⁷, A. Bilandzic ⁹⁶, G. Biro ¹³⁶, S. Biswas ⁴, N. Bize ¹⁰⁴, J.T. Blair ¹⁰⁸, D. Blau ¹⁴⁰, M.B. Blidaru ⁹⁸, N. Bluhme ³⁸, C. Blume ⁶³, G. Boca ^{21,54}, F. Bock ⁸⁷, T. Bodova ²⁰, A. Bogdanov ¹⁴⁰, S. Boi ²², J. Bok ⁵⁷, L. Boldizsár ¹³⁶, A. Bolozdynya ¹⁴⁰, M. Bombara ³⁷, P.M. Bond ³², G. Bonomi ^{131,54}, H. Borel ¹²⁸, A. Borissov ¹⁴⁰, H. Bossi ¹³⁷, E. Botta ²⁴, L. Bratrud ⁶³, P. Braun-Munzinger ⁹⁸, M. Bregant ¹¹⁰, M. Broz ³⁵, G.E. Bruno ^{97,31}, M.D. Buckland ¹¹⁷, D. Budnikov ¹⁴⁰, H. Buesching ⁶³, S. Bufalino ²⁹, O. Bugnon ¹⁰⁴, P. Buhler ¹⁰³, Z. Buthelezi ^{67,121}, J.B. Butt ¹³, A. Bylinkin ¹¹⁶, S.A. Bysiak ¹⁰⁷, M. Cai ^{27,6}, H. Caines ¹³⁷, A. Caliva ⁹⁸, E. Calvo Villar ¹⁰², J.M.M. Camacho ¹⁰⁹, P. Camerini ²³, F.D.M. Canedo ¹¹⁰, M. Carabas ¹²⁴, F. Carnesecchi ³², R. Caron ¹²⁶, J. Castillo Castellanos ¹²⁸, F. Catalano ^{24,29}, C. Ceballos Sanchez ¹⁴¹, I. Chakaberia ⁷⁴, P. Chakraborty ⁴⁶, S. Chandra ¹³², S. Chapelend ³², M. Chartier ¹¹⁷, S. Chattopadhyay ¹³², S. Chattopadhyay ¹⁰⁰, T.G. Chavez ⁴⁴, T. Cheng ⁶, C. Cheshkov ¹²⁶, B. Cheynis ¹²⁶, V. Chibante Barroso ³², D.D. Chinellato ¹¹¹, E.S. Chizzali ^{II,96}, J. Cho ⁵⁷, S. Cho ⁵⁷, P. Chochula ³², P. Christakoglou ⁸⁴, C.H. Christensen ⁸³, P. Christiansen ⁷⁵, T. Chujo ¹²³, M. Ciacco ²⁹, C. Cicalo ⁵¹, L. Cifarelli ²⁵, F. Cindolo ⁵⁰, M.R. Ciupé ⁹⁸, G. Clai^{III,50}, F. Colamaria ⁴⁹, J.S. Colburn ¹⁰¹, D. Colella ^{97,31}, A. Collu ⁷⁴, M. Colocci ³², M. Concas ^{IV,55}, G. Conesa Balbastre ⁷³, Z. Conesa del Valle ⁷², G. Contin ²³, J.G. Contreras ³⁵, M.L. Coquet ¹²⁸, T.M. Cormier ^{1,87}, P. Cortese ^{130,55}, M.R. Cosentino ¹¹², F. Costa ³², S. Costanza ^{21,54}, P. Crochet ¹²⁵, R. Cruz-Torres ⁷⁴, E. Cuautle ⁶⁴, P. Cui ⁶, L. Cunqueiro ⁸⁷, A. Dainese ⁵³, M.C. Danisch ⁹⁵, A. Danu ⁶², P. Das ⁸⁰, P. Das ⁴, S. Das ⁴, A.R. Dash ¹³⁵, S. Dash ⁴⁶, A. De Caro ²⁸, G. de Cataldo ⁴⁹, L. De Cilladi ²⁴, J. de Cuveland ³⁸, A. De Falco ²², D. De Gruttola ²⁸, N. De Marco ⁵⁵, C. De Martin ²³, S. De Pasquale ²⁸, S. Deb ⁴⁷, R.J. Debski ², K.R. Deja ¹³³, R. Del Grande ⁹⁶, L. Dello Stritto ²⁸, W. Deng ⁶, P. Dhankher ¹⁸, D. Di Bari ³¹, A. Di Mauro ³², R.A. Diaz ^{141,7}, T. Dietel ¹¹³, Y. Ding ^{126,6}, R. Divià ³², D.U. Dixit ¹⁸, Ø. Djupsland ²⁰, U. Dmitrieva ¹⁴⁰, A. Dobrin ⁶², B. Dönigus ⁶³, A.K. Dubey ¹³², J.M. Dubinski ¹³³, A. Dubla ⁹⁸, S. Dudi ⁹⁰, P. Dupieux ¹²⁵, M. Durkac ¹⁰⁶, N. Dzalaiova ¹², T.M. Eder ¹³⁵, R.J. Ehlers ⁸⁷, V.N. Eikeland ²⁰, F. Eisenhut ⁶³, D. Elia ⁴⁹, B. Erazmus ¹⁰⁴, F. Ercolelli ²⁵, F. Erhardt ⁸⁹, M.R. Ersdal ²⁰, B. Espagnon ⁷², G. Eulisse ³², D. Evans ¹⁰¹, S. Evdokimov ¹⁴⁰, L. Fabbietti ⁹⁶, M. Faggin ²⁷, J. Faivre ⁷³, F. Fan ⁶, W. Fan ⁷⁴, A. Fantoni ⁴⁸, M. Fasel ⁸⁷, P. Fecchio ²⁹, A. Feliciello ⁵⁵, G. Feofilov ¹⁴⁰, A. Fernández Téllez ⁴⁴, M.B. Ferrer ³², A. Ferrero ¹²⁸, C. Ferrero ⁵⁵, A. Ferretti ²⁴, V.J.G. Feuillard ⁹⁵, J. Figiel ¹⁰⁷, V. Filova ³⁵, D. Finogeev ¹⁴⁰, F.M. Fionda ⁵¹, G. Fiorenza ⁹⁷, F. Flor ¹¹⁴, A.N. Flores ¹⁰⁸, S. Foertsch ⁶⁷, I. Fokin ⁹⁵, S. Fokin ¹⁴⁰, E. Fragiocomo ⁵⁶, E. Frajna ¹³⁶, U. Fuchs ³², N. Funicello ²⁸, C. Furget ⁷³, A. Furs ¹⁴⁰, T. Fusayasu ⁹⁹, J.J. Gaardhøje ⁸³, M. Gagliardi ²⁴, A.M. Gago ¹⁰², A. Gal ¹²⁷, C.D. Galvan ¹⁰⁹, D.R. Gangadharan ¹¹⁴, P. Ganoti ⁷⁸, C. Garabatos ⁹⁸, J.R.A. Garcia ⁴⁴, E. Garcia-Solis ⁹, K. Garg ¹⁰⁴, C. Gargiulo ³², A. Garibaldi ⁸¹, K. Garner ¹³⁵, A. Gautam ¹¹⁶, M.B. Gay Ducati ⁶⁵, M. Germain ¹⁰⁴, C. Ghosh ¹³², S.K. Ghosh ⁴, M. Giacalone ²⁵, P. Gianotti ⁴⁸, P. Giubellino ^{98,55}, P. Giubilato ²⁷, A.M.C. Glaenzer ¹²⁸, P. Glässel ⁹⁵, E. Glimos ¹²⁰, D.J.Q. Goh ⁷⁶, V. Gonzalez ¹³⁴, L.H. González-Trueba ⁶⁶, M. Gorgon ², L. Görlich ¹⁰⁷, S. Gotovac ³³, V. Grabski ⁶⁶, L.K. Graczykowski ¹³³, E. Grecka ⁸⁶, L. Greiner ⁷⁴, A. Grelli ⁵⁸, C. Grigoras ³², V. Grigoriev ¹⁴⁰, S. Grigoryan ^{141,1}, F. Grossa ³², J.F. Grosse-Oetringhaus ³², R. Grossi ⁹⁸, D. Grund ³⁵, G.G. Guardiano ¹¹¹, R. Guernane ⁷³, M. Guilbaud ¹⁰⁴, K. Gulbrandsen ⁸³,

- T. Gunji ¹²², W. Guo ⁶, A. Gupta ⁹¹, R. Gupta ⁹¹, S.P. Guzman ⁴⁴, L. Gyulai ¹³⁶, M.K. Habib ⁹⁸, C. Hadjidakis ⁷², H. Hamagaki ⁷⁶, M. Hamid ⁶, Y. Han ¹³⁸, R. Hannigan ¹⁰⁸, M.R. Haque ¹³³, A. Harlenderova ⁹⁸, J.W. Harris ¹³⁷, A. Harton ⁹, H. Hassan ⁸⁷, D. Hatzifotiadou ⁵⁰, P. Hauer ⁴², L.B. Havener ¹³⁷, S.T. Heckel ⁹⁶, E. Hellbär ⁹⁸, H. Helstrup ³⁴, T. Herman ³⁵, G. Herrera Corral ⁸, F. Herrmann ¹³⁵, S. Hermann ¹²⁶, K.F. Hetland ³⁴, B. Heybeck ⁶³, H. Hillemanns ³², C. Hills ¹¹⁷, B. Hippolyte ¹²⁷, B. Hofman ⁵⁸, B. Hohlweger ⁸⁴, J. Honermann ¹³⁵, G.H. Hong ¹³⁸, D. Horak ³⁵, A. Horzyk ², R. Hosokawa ¹⁴, Y. Hou ⁶, P. Hristov ³², C. Hughes ¹²⁰, P. Huhn ⁶³, L.M. Huhta ¹¹⁵, C.V. Hulse ⁷², T.J. Humanic ⁸⁸, H. Hushnud ¹⁰⁰, A. Hutson ¹¹⁴, D. Hutter ³⁸, J.P. Iddon ¹¹⁷, R. Ilkaev ¹⁴⁰, H. Ilyas ¹³, M. Inaba ¹²³, G.M. Innocenti ³², M. Ippolitov ¹⁴⁰, A. Isakov ⁸⁶, T. Isidori ¹¹⁶, M.S. Islam ¹⁰⁰, M. Ivanov ¹², M. Ivanov ⁹⁸, V. Ivanov ¹⁴⁰, V. Izucheev ¹⁴⁰, M. Jablonski ², B. Jacak ⁷⁴, N. Jacazio ³², P.M. Jacobs ⁷⁴, S. Jadlovska ¹⁰⁶, J. Jadlovsky ¹⁰⁶, S. Jaelani ⁸², L. Jaffe ³⁸, C. Jahnke ¹¹¹, M.A. Janik ¹³³, T. Janson ⁶⁹, M. Jercic ⁸⁹, O. Jevons ¹⁰¹, A.A.P. Jimenez ⁶⁴, F. Jonas ⁸⁷, P.G. Jones ¹⁰¹, J.M. Jowett ^{32,98}, J. Jung ⁶³, M. Jung ⁶³, A. Junique ³², A. Jusko ¹⁰¹, M.J. Kabus ^{32,133}, J. Kaewjai ¹⁰⁵, P. Kalinak ⁵⁹, A.S. Kalteyer ⁹⁸, A. Kalweit ³², V. Kaplin ¹⁴⁰, A. Karasu Uysal ⁷¹, D. Karatovic ⁸⁹, O. Karavichev ¹⁴⁰, T. Karavicheva ¹⁴⁰, P. Karczmarczyk ¹³³, E. Karpechev ¹⁴⁰, V. Kashyap ⁸⁰, A. Kazantsev ¹⁴⁰, U. Kebschull ⁶⁹, R. Keidel ¹³⁹, D.L.D. Keijdener ⁵⁸, M. Keil ³², B. Ketzer ⁴², A.M. Khan ⁶, S. Khan ¹⁵, A. Khanzadeev ¹⁴⁰, Y. Kharlov ¹⁴⁰, A. Khatun ¹⁵, A. Khuntia ¹⁰⁷, B. Kileng ³⁴, B. Kim ¹⁶, C. Kim ¹⁶, D.J. Kim ¹¹⁵, E.J. Kim ⁶⁸, J. Kim ¹³⁸, J.S. Kim ⁴⁰, J. Kim ⁹⁵, J. Kim ⁶⁸, M. Kim ⁹⁵, S. Kim ¹⁷, T. Kim ¹³⁸, K. Kimura ⁹³, S. Kirsch ⁶³, I. Kisel ³⁸, S. Kiselev ¹⁴⁰, A. Kisiel ¹³³, J.P. Kitowski ², J.L. Klay ⁵, J. Klein ³², S. Klein ⁷⁴, C. Klein-Bösing ¹³⁵, M. Kleiner ⁶³, T. Klemenz ⁹⁶, A. Kluge ³², A.G. Knospe ¹¹⁴, C. Kobdaj ¹⁰⁵, T. Kollegger ⁹⁸, A. Kondratyev ¹⁴¹, E. Kondratyuk ¹⁴⁰, J. Konig ⁶³, S.A. Konigstorfer ⁹⁶, P.J. Konopka ³², G. Kornakov ¹³³, S.D. Koryciak ², A. Kotliarov ⁸⁶, O. Kovalenko ⁷⁹, V. Kovalenko ¹⁴⁰, M. Kowalski ¹⁰⁷, I. Králik ⁵⁹, A. Kravčáková ³⁷, L. Kreis ⁹⁸, M. Krivda ^{101,59}, F. Krizek ⁸⁶, K. Krizkova Gajdosova ³⁵, M. Kroesen ⁹⁵, M. Krüger ⁶³, D.M. Krupova ³⁵, E. Kryshen ¹⁴⁰, M. Krzewicki ³⁸, V. Kučera ³², C. Kuhn ¹²⁷, P.G. Kuijer ⁸⁴, T. Kumaoka ¹²³, D. Kumar ¹³², L. Kumar ⁹⁰, N. Kumar ⁹⁰, S. Kumar ³¹, S. Kundu ³², P. Kurashvili ⁷⁹, A. Kurepin ¹⁴⁰, A.B. Kurepin ¹⁴⁰, S. Kushpil ⁸⁶, J. Kvapil ¹⁰¹, M.J. Kweon ⁵⁷, J.Y. Kwon ⁵⁷, Y. Kwon ¹³⁸, S.L. La Pointe ³⁸, P. La Rocca ²⁶, Y.S. Lai ⁷⁴, A. Lakrathok ¹⁰⁵, M. Lamanna ³², R. Langoy ¹¹⁹, P. Larionov ⁴⁸, E. Laudi ³², L. Lautner ^{32,96}, R. Lavicka ¹⁰³, T. Lazareva ¹⁴⁰, R. Lea ^{131,54}, G. Legras ¹³⁵, J. Lehrbach ³⁸, R.C. Lemmon ⁸⁵, I. León Monzón ¹⁰⁹, M.M. Lesch ⁹⁶, E.D. Lesser ¹⁸, M. Lettrich ⁹⁶, P. Lévai ¹³⁶, X. Li ¹⁰, X.L. Li ⁶, J. Lien ¹¹⁹, R. Lietava ¹⁰¹, B. Lim ¹⁶, S.H. Lim ¹⁶, V. Lindenstruth ³⁸, A. Lindner ⁴⁵, C. Lippmann ⁹⁸, A. Liu ¹⁸, D.H. Liu ⁶, J. Liu ¹¹⁷, I.M. Lofnes ²⁰, C. Loizides ⁸⁷, P. Loncar ³³, J.A. Lopez ⁹⁵, X. Lopez ¹²⁵, E. López Torres ⁷, P. Lu ^{98,118}, J.R. Luhder ¹³⁵, M. Lunardon ²⁷, G. Luparello ⁵⁶, Y.G. Ma ³⁹, A. Maevskaya ¹⁴⁰, M. Mager ³², T. Mahmoud ⁴², A. Maire ¹²⁷, M. Malaev ¹⁴⁰, G. Malfattore ²⁵, N.M. Malik ⁹¹, Q.W. Malik ¹⁹, S.K. Malik ⁹¹, L. Malinina ^{VII,141}, D. Mal'Kevich ¹⁴⁰, D. Mallick ⁸⁰, N. Mallick ⁴⁷, G. Mandaglio ^{30,52}, V. Manko ¹⁴⁰, F. Manso ¹²⁵, V. Manzari ⁴⁹, Y. Mao ⁶, G.V. Margagliotti ²³, A. Margotti ⁵⁰, A. Marín ⁹⁸, C. Markert ¹⁰⁸, M. Marquard ⁶³, P. Martinengo ³², J.L. Martinez ¹¹⁴, M.I. Martínez ⁴⁴, G. Martínez García ¹⁰⁴, S. Masciocchi ⁹⁸, M. Masera ²⁴, A. Masoni ⁵¹, L. Massacrier ⁷², A. Mastroserio ^{129,49}, A.M. Mathis ⁹⁶, O. Matonoha ⁷⁵, P.F.T. Matuoka ¹¹⁰, A. Matyja ¹⁰⁷, C. Mayer ¹⁰⁷, A.L. Mazuecos ³², F. Mazzaschi ²⁴, M. Mazzilli ³², J.E. Mdhluli ¹²¹, A.F. Mechler ⁶³, Y. Melikyan ¹⁴⁰, A. Menchaca-Rocha ⁶⁶, E. Meninno ^{103,28}, A.S. Menon ¹¹⁴, M. Meres ¹², S. Mhlanga ^{113,67}, Y. Miake ¹²³, L. Micheletti ⁵⁵, L.C. Migliorin ¹²⁶, D.L. Mihaylov ⁹⁶, K. Mikhaylov ^{141,140}, A.N. Mishra ¹³⁶, D. Miśkowiec ⁹⁸, A. Modak ⁴, A.P. Mohanty ⁵⁸, B. Mohanty ⁸⁰, M. Mohisin Khan ^{V,15}, M.A. Molander ⁴³, Z. Moravcova ⁸³, C. Mordasini ⁹⁶, D.A. Moreira De Godoy ¹³⁵, I. Morozov ¹⁴⁰, A. Morsch ³², T. Mrnjavac ³², V. Muccifora ⁴⁸, S. Muhuri ¹³², J.D. Mulligan ⁷⁴, A. Mulliri ²², M.G. Munhoz ¹¹⁰, R.H. Munzer ⁶³, H. Murakami ¹²², S. Murray ¹¹³, L. Musa ³², J. Musinsky ⁵⁹, J.W. Myrcha ¹³³, B. Naik ¹²¹, R. Nair ⁷⁹, A.I. Nambrath ¹⁸, B.K. Nandi ⁴⁶, R. Nania ⁵⁰, E. Nappi ⁴⁹, A.F. Nassirpour ⁷⁵, A. Nath ⁹⁵, C. Nattrass ¹²⁰, A. Neagu ¹⁹, A. Negru ¹²⁴, L. Nellen ⁶⁴, S.V. Nesbo ³⁴, G. Neskovic ³⁸, D. Nesterov ¹⁴⁰, B.S. Nielsen ⁸³, E.G. Nielsen ⁸³, S. Nikolaev ¹⁴⁰, S. Nikulin ¹⁴⁰, V. Nikulin ¹⁴⁰, F. Noferini ⁵⁰, S. Noh ¹¹, P. Nomokonov ¹⁴¹, J. Norman ¹¹⁷, N. Novitzky ¹²³, P. Nowakowski ¹³³, A. Nyandin ¹⁴⁰, J. Nystrand ²⁰, M. Ogino ⁷⁶, A. Ohlson ⁷⁵, V.A. Okorokov ¹⁴⁰, J. Oleniacz ¹³³, A.C. Oliveira Da Silva ¹²⁰, M.H. Oliver ¹³⁷, A. Onnerstad ¹¹⁵, C. Oppedisano ⁵⁵, A. Ortiz Velasquez ⁶⁴, A. Oskarsson ⁷⁵, J. Otwinowski ¹⁰⁷, M. Oya ⁹³, K. Oyama ⁷⁶, Y. Pachmayer ⁹⁵, S. Padhan ⁴⁶, D. Pagano ^{131,54}, G. Paić ⁶⁴, A. Palasciano ⁴⁹, S. Panebianco ¹²⁸, H. Park ¹²³, J. Park ⁵⁷, J.E. Parkkila ^{32,115}, S.P. Pathak ¹¹⁴, R.N. Patra ⁹¹, B. Paul ²²,

- H. Pei ⁶, T. Peitzmann ⁵⁸, X. Peng ⁶, M. Pennisi ²⁴, L.G. Pereira ⁶⁵, H. Pereira Da Costa ¹²⁸, D. Peresunko ¹⁴⁰, G.M. Perez ⁷, S. Perrin ¹²⁸, Y. Pestov¹⁴⁰, V. Petráček ³⁵, V. Petrov ¹⁴⁰, M. Petrovici ⁴⁵, R.P. Pezzi ^{104,65}, S. Piano ⁵⁶, M. Pikna ¹², P. Pillot ¹⁰⁴, O. Pinazza ^{50,32}, L. Pinsky¹¹⁴, C. Pinto ⁹⁶, S. Pisano ⁴⁸, M. Płoskoń ⁷⁴, M. Planinic⁸⁹, F. Pliquet ⁶³, M.G. Poghosyan ⁸⁷, S. Politano ²⁹, N. Poljak ⁸⁹, A. Pop ⁴⁵, S. Porteboeuf-Houssais ¹²⁵, J. Porter ⁷⁴, V. Pozdniakov ¹⁴¹, S.K. Prasad ⁴, S. Prasad ⁴⁷, R. Preghenella ⁵⁰, F. Prino ⁵⁵, C.A. Pruneau ¹³⁴, I. Pshenichnov ¹⁴⁰, M. Puccio ³², S. Pucillo ²⁴, Z. Pugelova¹⁰⁶, S. Qiu ⁸⁴, L. Quaglia ²⁴, R.E. Quishpe¹¹⁴, S. Ragoni ¹⁰¹, A. Rakotozafindrabe ¹²⁸, L. Ramello ^{130,55}, F. Rami ¹²⁷, S.A.R. Ramirez ⁴⁴, T.A. Rancien ⁷³, R. Raniwala ⁹², S. Raniwala⁹², S.S. Räsänen ⁴³, R. Rath ^{50,47}, I. Ravasenga ⁸⁴, K.F. Read ^{87,120}, A.R. Redelbach ³⁸, K. Redlich ^{VI,79}, A. Rehman²⁰, P. Reichelt ⁶³, F. Reidt ³², H.A. Reme-Ness ³⁴, Z. Rescakova³⁷, K. Reygers ⁹⁵, A. Riabov ¹⁴⁰, V. Riabov ¹⁴⁰, R. Ricci ²⁸, T. Richert ⁷⁵, M. Richter ¹⁹, A.A. Riedel ⁹⁶, W. Riegler ³², F. Riggi ²⁶, C. Ristea ⁶², M. Rodríguez Cahuantzi ⁴⁴, K. Røed ¹⁹, R. Rogalev ¹⁴⁰, E. Rogochaya ¹⁴¹, T.S. Rogoschinski ⁶³, D. Rohr ³², D. Röhrich ²⁰, P.F. Rojas⁴⁴, S. Rojas Torres ³⁵, P.S. Rokita ¹³³, G. Romanenko ¹⁴¹, F. Ronchetti ⁴⁸, A. Rosano ^{30,52}, E.D. Rosas⁶⁴, A. Rossi ⁵³, A. Roy ⁴⁷, P. Roy¹⁰⁰, S. Roy⁴⁶, N. Rubini ²⁵, O.V. Rueda ⁷⁵, D. Ruggiano ¹³³, R. Rui ²³, B. Rumyantsev¹⁴¹, P.G. Russek ², R. Russo ⁸⁴, A. Rustamov ⁸¹, E. Ryabinkin ¹⁴⁰, Y. Ryabov ¹⁴⁰, A. Rybicki ¹⁰⁷, H. Rytkonen ¹¹⁵, W. Rzesz ¹³³, O.A.M. Saarimaki ⁴³, R. Sadek ¹⁰⁴, S. Sadhu ³¹, S. Sadovsky ¹⁴⁰, J. Saetre ²⁰, K. Šafařík ³⁵, S. Saha ⁸⁰, B. Sahoo ⁴⁶, R. Sahoo ⁴⁷, S. Sahoo⁶⁰, D. Sahu ⁴⁷, P.K. Sahu ⁶⁰, J. Saini ¹³², K. Sajdakova³⁷, S. Sakai ¹²³, M.P. Salvan ⁹⁸, S. Sambyal ⁹¹, T.B. Saramela¹¹⁰, D. Sarkar ¹³⁴, N. Sarkar¹³², P. Sarma⁴¹, V. Sarritzu ²², V.M. Sarti ⁹⁶, M.H.P. Sas ¹³⁷, J. Schambach ⁸⁷, H.S. Scheid ⁶³, C. Schiaua ⁴⁵, R. Schicker ⁹⁵, A. Schmah ⁹⁵, C. Schmidt ⁹⁸, H.R. Schmidt ⁹⁴, M.O. Schmidt ³², M. Schmidt ⁹⁴, N.V. Schmidt ⁸⁷, A.R. Schmier ¹²⁰, R. Schotter ¹²⁷, J. Schukraft ³², K. Schwarz ⁹⁸, K. Schweda ⁹⁸, G. Scioli ²⁵, E. Scomparin ⁵⁵, J.E. Seger ¹⁴, Y. Sekiguchi¹²², D. Sekihata ¹²², I. Selyuzhenkov ^{98,140}, S. Senyukov ¹²⁷, J.J. Seo ⁵⁷, D. Serebryakov ¹⁴⁰, L. Šerkšnytė ⁹⁶, A. Sevcenco ⁶², T.J. Shaba ⁶⁷, A. Shabetai ¹⁰⁴, R. Shahoyan³², A. Shangaraev ¹⁴⁰, A. Sharma ⁹⁰, D. Sharma ⁴⁶, H. Sharma ¹⁰⁷, M. Sharma ⁹¹, N. Sharma⁹⁰, S. Sharma ⁷⁶, S. Sharma ⁹¹, U. Sharma ⁹¹, A. Shatat ⁷², O. Sheibani¹¹⁴, K. Shigaki ⁹³, M. Shimomura⁷⁷, S. Shirinkin ¹⁴⁰, Q. Shou ³⁹, Y. Sibiriak ¹⁴⁰, S. Siddhanta ⁵¹, T. Siemiarczuk ⁷⁹, T.F. Silva ¹¹⁰, D. Silvermyr ⁷⁵, T. Simantathammakul¹⁰⁵, R. Simeonov ³⁶, G. Simonetti³², B. Singh ⁹¹, B. Singh ⁹⁶, R. Singh ⁸⁰, R. Singh ⁹¹, R. Singh ⁴⁷, S. Singh ¹⁵, V.K. Singh ¹³², V. Singhal ¹³², T. Sinha ¹⁰⁰, B. Sitar ¹², M. Sitta ^{130,55}, T.B. Skaali¹⁹, G. Skorodumovs ⁹⁵, M. Slupecki ⁴³, N. Smirnov ¹³⁷, R.J.M. Snellings ⁵⁸, E.H. Solheim ¹⁹, C. Soncco¹⁰², J. Song ¹¹⁴, A. Songmoolnak¹⁰⁵, F. Soramel ²⁷, S. Sorensen ¹²⁰, R. Spijkers ⁸⁴, I. Sputowska ¹⁰⁷, J. Staa ⁷⁵, J. Stachel ⁹⁵, I. Stan ⁶², P.J. Steffanic ¹²⁰, S.F. Stiefelmaier ⁹⁵, D. Stocco ¹⁰⁴, I. Storehaug ¹⁹, M.M. Storetvedt ³⁴, P. Stratmann ¹³⁵, S. Strazzi ²⁵, C.P. Stylianidis⁸⁴, A.A.P. Suaide ¹¹⁰, C. Suire ⁷², M. Sukhanov ¹⁴⁰, M. Suljic ³², V. Sumberia ⁹¹, S. Sumowidagdo ⁸², S. Swain ⁶⁰, I. Szarka ¹², U. Tabassam¹³, S.F. Taghavi ⁹⁶, G. Taillepied ⁹⁸, J. Takahashi ¹¹¹, G.J. Tambave ²⁰, S. Tang ^{125,6}, Z. Tang ¹¹⁸, J.D. Tapia Takaki ¹¹⁶, N. Tapus¹²⁴, L.A. Tarasovicova ¹³⁵, M.G. Tarzila ⁴⁵, G.F. Tassielli ³¹, A. Tauro ³², A. Telesca ³², L. Terlizzi ²⁴, C. Terrevoli ¹¹⁴, G. Tersimonov³, D. Thomas ¹⁰⁸, A. Tikhonov ¹⁴⁰, A.R. Timmins ¹¹⁴, M. Tkacik¹⁰⁶, T. Tkacik ¹⁰⁶, A. Toia ⁶³, R. Tokumoto⁹³, N. Topilskaya ¹⁴⁰, M. Toppi ⁴⁸, F. Torales-Acosta¹⁸, T. Tork ⁷², A.G. Torres Ramos ³¹, A. Trifiró ^{30,52}, A.S. Triolo ^{30,52}, S. Tripathy ⁵⁰, T. Tripathy ⁴⁶, S. Trogolo ³², V. Trubnikov ³, W.H. Trzaska ¹¹⁵, T.P. Trzciński ¹³³, R. Turrisi ⁵³, T.S. Tveter ¹⁹, K. Ullaland ²⁰, B. Ulukutlu ⁹⁶, A. Uras ¹²⁶, M. Urioni ^{54,131}, G.L. Usai ²², M. Vala³⁷, N. Valle ²¹, S. Vallero ⁵⁵, L.V.R. van Doremalen⁵⁸, M. van Leeuwen ⁸⁴, C.A. van Veen ⁹⁵, R.J.G. van Weelden ⁸⁴, P. Vande Vyvre ³², D. Varga ¹³⁶, Z. Varga ¹³⁶, M. Varga-Kofaragoğlu ¹³⁶, M. Vasileiou ⁷⁸, A. Vasiliev ¹⁴⁰, O. Vázquez Doce ⁹⁶, V. Vechernin ¹⁴⁰, E. Vercellin ²⁴, S. Vergara Limón⁴⁴, L. Vermunt ⁹⁸, R. Vértesi ¹³⁶, M. Verweij ⁵⁸, L. Vickovic³³, Z. Vilakazi¹²¹, O. Villalobos Baillie ¹⁰¹, G. Vino ⁴⁹, A. Vinogradov ¹⁴⁰, T. Virgili ²⁸, V. Vislavicius⁸³, A. Vodopyanov ¹⁴¹, B. Volkel ³², M.A. Völkli ⁹⁵, K. Voloshin¹⁴⁰, S.A. Voloshin ¹³⁴, G. Volpe ³¹, B. von Haller ³², I. Vorobyev ⁹⁶, N. Vozniuk ¹⁴⁰, J. Vrláková ³⁷, B. Wagner²⁰, C. Wang ³⁹, D. Wang³⁹, M. Weber ¹⁰³, A. Wegrzynek ³², F.T. Weighofer³⁸, S.C. Wenzel ³², J.P. Wessels ¹³⁵, S.L. Weyhmiller ¹³⁷, J. Wiechula ⁶³, J. Wikne ¹⁹, G. Wilk ⁷⁹, J. Wilkinson ⁹⁸, G.A. Willems ¹³⁵, B. Windelband⁹⁵, M. Winn ¹²⁸, J.R. Wright ¹⁰⁸, W. Wu³⁹, Y. Wu ¹¹⁸, R. Xu ⁶, A. Yadav ⁴², A.K. Yadav ¹³², S. Yalcin ⁷¹, Y. Yamaguchi⁹³, K. Yamakawa⁹³, S. Yang²⁰, S. Yano ⁹³, Z. Yin ⁶, I.-K. Yoo ¹⁶, J.H. Yoon ⁵⁷, S. Yuan²⁰, A. Yuncu ⁹⁵, V. Zaccolo ²³, C. Zampolli ³², H.J.C. Zanolí⁵⁸, F. Zanone ⁹⁵, N. Zardoshti ^{32,101}, A. Zarochentsev ¹⁴⁰, P. Závada ⁶¹, N. Zaviyalov ¹⁴⁰, M. Zhalov ¹⁴⁰, B. Zhang ⁶, S. Zhang ³⁹, X. Zhang ¹⁸, Y. Zhang ¹¹⁸, Z. Zhang ⁶,

M. Zhao¹⁰, V. Zherebchevskii¹⁴⁰, Y. Zhi¹⁰, N. Zhigareva¹⁴⁰, D. Zhou⁶, Y. Zhou⁸³, J. Zhu^{98,6}, Y. Zhu⁶, G. Zinovjev^{1,3}, N. Zurlo^{131,54}

Affiliation Notes

^I Deceased

^{II} Also at: Max-Planck-Institut für Physik, Munich, Germany

^{III} Also at: Italian National Agency for New Technologies, Energy and Sustainable Economic Development (ENEA), Bologna, Italy

^{IV} Also at: Dipartimento DET del Politecnico di Torino, Turin, Italy

^V Also at: Department of Applied Physics, Aligarh Muslim University, Aligarh, India

^{VI} Also at: Institute of Theoretical Physics, University of Wroclaw, Poland

^{VII} Also at: An institution covered by a cooperation agreement with CERN

Collaboration Institutes

¹ A.I. Alikhanyan National Science Laboratory (Yerevan Physics Institute) Foundation, Yerevan, Armenia

² AGH University of Science and Technology, Cracow, Poland

³ Bogolyubov Institute for Theoretical Physics, National Academy of Sciences of Ukraine, Kiev, Ukraine

⁴ Bose Institute, Department of Physics and Centre for Astroparticle Physics and Space Science (CAPSS), Kolkata, India

⁵ California Polytechnic State University, San Luis Obispo, California, United States

⁶ Central China Normal University, Wuhan, China

⁷ Centro de Aplicaciones Tecnológicas y Desarrollo Nuclear (CEADEN), Havana, Cuba

⁸ Centro de Investigación y de Estudios Avanzados (CINVESTAV), Mexico City and Mérida, Mexico

⁹ Chicago State University, Chicago, Illinois, United States

¹⁰ China Institute of Atomic Energy, Beijing, China

¹¹ Chungbuk National University, Cheongju, Republic of Korea

¹² Comenius University Bratislava, Faculty of Mathematics, Physics and Informatics, Bratislava, Slovak Republic

¹³ COMSATS University Islamabad, Islamabad, Pakistan

¹⁴ Creighton University, Omaha, Nebraska, United States

¹⁵ Department of Physics, Aligarh Muslim University, Aligarh, India

¹⁶ Department of Physics, Pusan National University, Pusan, Republic of Korea

¹⁷ Department of Physics, Sejong University, Seoul, Republic of Korea

¹⁸ Department of Physics, University of California, Berkeley, California, United States

¹⁹ Department of Physics, University of Oslo, Oslo, Norway

²⁰ Department of Physics and Technology, University of Bergen, Bergen, Norway

²¹ Dipartimento di Fisica, Università di Pavia, Pavia, Italy

²² Dipartimento di Fisica dell’Università and Sezione INFN, Cagliari, Italy

²³ Dipartimento di Fisica dell’Università and Sezione INFN, Trieste, Italy

²⁴ Dipartimento di Fisica dell’Università and Sezione INFN, Turin, Italy

²⁵ Dipartimento di Fisica e Astronomia dell’Università and Sezione INFN, Bologna, Italy

²⁶ Dipartimento di Fisica e Astronomia dell’Università and Sezione INFN, Catania, Italy

²⁷ Dipartimento di Fisica e Astronomia dell’Università and Sezione INFN, Padova, Italy

²⁸ Dipartimento di Fisica ‘E.R. Caianiello’ dell’Università and Gruppo Collegato INFN, Salerno, Italy

²⁹ Dipartimento DISAT del Politecnico and Sezione INFN, Turin, Italy

³⁰ Dipartimento di Scienze MIFT, Università di Messina, Messina, Italy

³¹ Dipartimento Interateneo di Fisica ‘M. Merlin’ and Sezione INFN, Bari, Italy

³² European Organization for Nuclear Research (CERN), Geneva, Switzerland

³³ Faculty of Electrical Engineering, Mechanical Engineering and Naval Architecture, University of Split, Split, Croatia

³⁴ Faculty of Engineering and Science, Western Norway University of Applied Sciences, Bergen, Norway

³⁵ Faculty of Nuclear Sciences and Physical Engineering, Czech Technical University in Prague, Prague, Czech Republic

³⁶ Faculty of Physics, Sofia University, Sofia, Bulgaria

³⁷ Faculty of Science, P.J. Šafárik University, Košice, Slovak Republic

- ³⁸ Frankfurt Institute for Advanced Studies, Johann Wolfgang Goethe-Universität Frankfurt, Frankfurt, Germany
³⁹ Fudan University, Shanghai, China
⁴⁰ Gangneung-Wonju National University, Gangneung, Republic of Korea
⁴¹ Gauhati University, Department of Physics, Guwahati, India
⁴² Helmholtz-Institut für Strahlen- und Kernphysik, Rheinische Friedrich-Wilhelms-Universität Bonn, Bonn, Germany
⁴³ Helsinki Institute of Physics (HIP), Helsinki, Finland
⁴⁴ High Energy Physics Group, Universidad Autónoma de Puebla, Puebla, Mexico
⁴⁵ Horia Hulubei National Institute of Physics and Nuclear Engineering, Bucharest, Romania
⁴⁶ Indian Institute of Technology Bombay (IIT), Mumbai, India
⁴⁷ Indian Institute of Technology Indore, Indore, India
⁴⁸ INFN, Laboratori Nazionali di Frascati, Frascati, Italy
⁴⁹ INFN, Sezione di Bari, Bari, Italy
⁵⁰ INFN, Sezione di Bologna, Bologna, Italy
⁵¹ INFN, Sezione di Cagliari, Cagliari, Italy
⁵² INFN, Sezione di Catania, Catania, Italy
⁵³ INFN, Sezione di Padova, Padova, Italy
⁵⁴ INFN, Sezione di Pavia, Pavia, Italy
⁵⁵ INFN, Sezione di Torino, Turin, Italy
⁵⁶ INFN, Sezione di Trieste, Trieste, Italy
⁵⁷ Inha University, Incheon, Republic of Korea
⁵⁸ Institute for Gravitational and Subatomic Physics (GRASP), Utrecht University/Nikhef, Utrecht, Netherlands
⁵⁹ Institute of Experimental Physics, Slovak Academy of Sciences, Košice, Slovak Republic
⁶⁰ Institute of Physics, Homi Bhabha National Institute, Bhubaneswar, India
⁶¹ Institute of Physics of the Czech Academy of Sciences, Prague, Czech Republic
⁶² Institute of Space Science (ISS), Bucharest, Romania
⁶³ Institut für Kernphysik, Johann Wolfgang Goethe-Universität Frankfurt, Frankfurt, Germany
⁶⁴ Instituto de Ciencias Nucleares, Universidad Nacional Autónoma de México, Mexico City, Mexico
⁶⁵ Instituto de Física, Universidade Federal do Rio Grande do Sul (UFRGS), Porto Alegre, Brazil
⁶⁶ Instituto de Física, Universidad Nacional Autónoma de México, Mexico City, Mexico
⁶⁷ iThemba LABS, National Research Foundation, Somerset West, South Africa
⁶⁸ Jeonbuk National University, Jeonju, Republic of Korea
⁶⁹ Johann-Wolfgang-Goethe Universität Frankfurt Institut für Informatik, Fachbereich Informatik und Mathematik, Frankfurt, Germany
⁷⁰ Korea Institute of Science and Technology Information, Daejeon, Republic of Korea
⁷¹ KTO Karatay University, Konya, Turkey
⁷² Laboratoire de Physique des 2 Infinis, Irène Joliot-Curie, Orsay, France
⁷³ Laboratoire de Physique Subatomique et de Cosmologie, Université Grenoble-Alpes, CNRS-IN2P3, Grenoble, France
⁷⁴ Lawrence Berkeley National Laboratory, Berkeley, California, United States
⁷⁵ Lund University Department of Physics, Division of Particle Physics, Lund, Sweden
⁷⁶ Nagasaki Institute of Applied Science, Nagasaki, Japan
⁷⁷ Nara Women's University (NWU), Nara, Japan
⁷⁸ National and Kapodistrian University of Athens, School of Science, Department of Physics , Athens, Greece
⁷⁹ National Centre for Nuclear Research, Warsaw, Poland
⁸⁰ National Institute of Science Education and Research, Homi Bhabha National Institute, Jatni, India
⁸¹ National Nuclear Research Center, Baku, Azerbaijan
⁸² National Research and Innovation Agency - BRIN, Jakarta, Indonesia
⁸³ Niels Bohr Institute, University of Copenhagen, Copenhagen, Denmark
⁸⁴ Nikhef, National institute for subatomic physics, Amsterdam, Netherlands
⁸⁵ Nuclear Physics Group, STFC Daresbury Laboratory, Daresbury, United Kingdom
⁸⁶ Nuclear Physics Institute of the Czech Academy of Sciences, Husinec-Řež, Czech Republic
⁸⁷ Oak Ridge National Laboratory, Oak Ridge, Tennessee, United States
⁸⁸ Ohio State University, Columbus, Ohio, United States
⁸⁹ Physics department, Faculty of science, University of Zagreb, Zagreb, Croatia
⁹⁰ Physics Department, Panjab University, Chandigarh, India

- ⁹¹ Physics Department, University of Jammu, Jammu, India
⁹² Physics Department, University of Rajasthan, Jaipur, India
⁹³ Physics Program and International Institute for Sustainability with Knotted Chiral Meta Matter (SKCM2), Hiroshima University, Hiroshima, Japan
⁹⁴ Physikalisches Institut, Eberhard-Karls-Universität Tübingen, Tübingen, Germany
⁹⁵ Physikalisches Institut, Ruprecht-Karls-Universität Heidelberg, Heidelberg, Germany
⁹⁶ Physik Department, Technische Universität München, Munich, Germany
⁹⁷ Politecnico di Bari and Sezione INFN, Bari, Italy
⁹⁸ Research Division and ExtreMe Matter Institute EMMI, GSI Helmholtzzentrum für Schwerionenforschung GmbH, Darmstadt, Germany
⁹⁹ Saga University, Saga, Japan
¹⁰⁰ Saha Institute of Nuclear Physics, Homi Bhabha National Institute, Kolkata, India
¹⁰¹ School of Physics and Astronomy, University of Birmingham, Birmingham, United Kingdom
¹⁰² Sección Física, Departamento de Ciencias, Pontificia Universidad Católica del Perú, Lima, Peru
¹⁰³ Stefan Meyer Institut für Subatomare Physik (SMI), Vienna, Austria
¹⁰⁴ SUBATECH, IMT Atlantique, Nantes Université, CNRS-IN2P3, Nantes, France
¹⁰⁵ Suranaree University of Technology, Nakhon Ratchasima, Thailand
¹⁰⁶ Technical University of Košice, Košice, Slovak Republic
¹⁰⁷ The Henryk Niewodniczanski Institute of Nuclear Physics, Polish Academy of Sciences, Cracow, Poland
¹⁰⁸ The University of Texas at Austin, Austin, Texas, United States
¹⁰⁹ Universidad Autónoma de Sinaloa, Culiacán, Mexico
¹¹⁰ Universidade de São Paulo (USP), São Paulo, Brazil
¹¹¹ Universidade Estadual de Campinas (UNICAMP), Campinas, Brazil
¹¹² Universidade Federal do ABC, Santo Andre, Brazil
¹¹³ University of Cape Town, Cape Town, South Africa
¹¹⁴ University of Houston, Houston, Texas, United States
¹¹⁵ University of Jyväskylä, Jyväskylä, Finland
¹¹⁶ University of Kansas, Lawrence, Kansas, United States
¹¹⁷ University of Liverpool, Liverpool, United Kingdom
¹¹⁸ University of Science and Technology of China, Hefei, China
¹¹⁹ University of South-Eastern Norway, Kongsberg, Norway
¹²⁰ University of Tennessee, Knoxville, Tennessee, United States
¹²¹ University of the Witwatersrand, Johannesburg, South Africa
¹²² University of Tokyo, Tokyo, Japan
¹²³ University of Tsukuba, Tsukuba, Japan
¹²⁴ University Politehnica of Bucharest, Bucharest, Romania
¹²⁵ Université Clermont Auvergne, CNRS/IN2P3, LPC, Clermont-Ferrand, France
¹²⁶ Université de Lyon, CNRS/IN2P3, Institut de Physique des 2 Infinis de Lyon, Lyon, France
¹²⁷ Université de Strasbourg, CNRS, IPHC UMR 7178, F-67000 Strasbourg, France, Strasbourg, France
¹²⁸ Université Paris-Saclay Centre d'Etudes de Saclay (CEA), IRFU, Département de Physique Nucléaire (DPhN), Saclay, France
¹²⁹ Università degli Studi di Foggia, Foggia, Italy
¹³⁰ Università del Piemonte Orientale, Vercelli, Italy
¹³¹ Università di Brescia, Brescia, Italy
¹³² Variable Energy Cyclotron Centre, Homi Bhabha National Institute, Kolkata, India
¹³³ Warsaw University of Technology, Warsaw, Poland
¹³⁴ Wayne State University, Detroit, Michigan, United States
¹³⁵ Westfälische Wilhelms-Universität Münster, Institut für Kernphysik, Münster, Germany
¹³⁶ Wigner Research Centre for Physics, Budapest, Hungary
¹³⁷ Yale University, New Haven, Connecticut, United States
¹³⁸ Yonsei University, Seoul, Republic of Korea
¹³⁹ Zentrum für Technologie und Transfer (ZTT), Worms, Germany
¹⁴⁰ Affiliated with an institute covered by a cooperation agreement with CERN
¹⁴¹ Affiliated with an international laboratory covered by a cooperation agreement with CERN.